

THREE-DIMENSIONAL GAUSSIAN BEAM SCATTERING FROM A PERIODIC SEQUENCE OF BI-ISOTROPIC AND MATERIAL LAYERS

V. Tuz

Department of Theoretical Radio Physics
Kharkov National University
Svobody Sq. 4, Kharkov, 61077, Ukraine

Abstract—The three-dimensional Gaussian beam scattering from the bounded periodic sequence of one-to-one composed isotropic magnetodielectric and bi-isotropic layers are investigated. The beam field is represented by an angular continuous spectrum of plane wave. The problem of the partial plane wave diffraction on the structure is solved using the circuit theory and the transfer matrix methods. It is found that after reflection from the structure, the circular Gaussian beam becomes, in general, an elliptical Gaussian beam, in addition to a displacement of the beam axis from the position predicted by ray optics.

1. INTRODUCTION

For solving many diffraction problems the simple plane waves are employed. In practice, a simple plane wave is not an option, but must be approximated by a beam of radiation, which can be modeled as it is in the present paper by a Gaussian beam [1, 2].

The problem of reflection and transmission of a wave beam from single isotropic and anisotropic layers, metal-dielectric heterogeneities and their periodical sequences has been the subject of numerous research papers [1–12]. Several beam-wave phenomena such as lateral shift, focal shift, angular shift, beam splitting that are not found in the reflection of plane wave are the major features for investigation. Papers [13–20] are devoted to investigate the wave beam scattering on the structures with the spatial dispersion that include single layers of the natural and artificial reciprocal (chiral) and nonreciprocal bi-isotropic, bi-anisotropic medium, gyrotropic crystals, etc. Most of these studies were based on a two-dimensional beam-wave structure. The reason for

this choice was perhaps the confidence that essential insights would not be lost while mathematical complexities could be reduced. However, it was shown in [5, 20] that this confidence may not be warranted, in particular, the two-dimensional model is not to take into consideration the polarization effects and not able to predict the change in ellipticity of the scattered beam.

In the present work the scattered fields of a three-dimensional Gaussian beam on a bounded periodical sequence of one-to-one composed isotropic magnetodielectric and bi-isotropic layers are investigated. The scattering coefficients of the plane monochromatic waves are determined using the circuit theory and the transfer matrix methods [21–25] and the beam field is represented by the angular continuous spectrum of the plane wave [1, 2, 9, 20].

The aim of this work is the performance improvement and functionality expansion for the electromagnetic field systems based on the exploitation of the media chirality [26–37].

2. PROBLEM FORMULATION

A periodic in the z -axis direction, with period L , structure of N identical basic elements (periods) is investigated (Fig. 1). Each of periods includes a homogeneous magnetodielectric and bi-isotropic layers with thicknesses d_1 and d_2 ($L = d_1 + d_2$) that are defined with the material parameters ε_1, μ_1 and $\varepsilon_2, \mu_2, \xi, \zeta$, respectively (ξ, ζ are the magnetoelectric interaction parameters). In general, the parameters ε_1, μ_1 and $\varepsilon_2, \mu_2, \xi, \zeta$, can be frequency dependent and complex for loss media. The outer half-spaces $z \leq 0$ and $z \geq NL$ are homogeneous, isotropic and have permittivities ε_0, μ_0 and ε_3, μ_3 , respectively.

Note that if $\xi = \zeta = 0$ (i.e., the both of layers are conventional materials), then the structure in Fig. 1 is known as a distributed Bragg reflector (DBR) [23].

The auxiliary coordinate system x_{in}, y_{in}, z_{in} is introduced for an incident beam field description [9]. In it, the incident field $\mathbf{E}_{in}, \mathbf{H}_{in}$ is written as the continued sum of the plane waves with the spectral parameter $\boldsymbol{\kappa}_{in}$ (it has a sense of the transverse wave vector of the partial plane wave):

$$\begin{aligned} \mathbf{E}_{in} &= \mathbf{e}_{in} \int \int_{-\infty}^{\infty} U(\boldsymbol{\kappa}_{in}) \exp(i\boldsymbol{\kappa}_{in} \cdot (\mathbf{r}_{in} + \mathbf{a}_{in}) + i\gamma_{in}(z_{in} + a_3)) d\boldsymbol{\kappa}_{in}, \\ \mathbf{H}_{in} &= \mathbf{h}_{in} \int \int_{-\infty}^{\infty} U(\boldsymbol{\kappa}_{in}) \exp(i\boldsymbol{\kappa}_{in} \cdot (\mathbf{r}_{in} + \mathbf{a}_{in}) + i\gamma_{in}(z_{in} + a_3)) d\boldsymbol{\kappa}_{in}, \end{aligned} \quad (1)$$

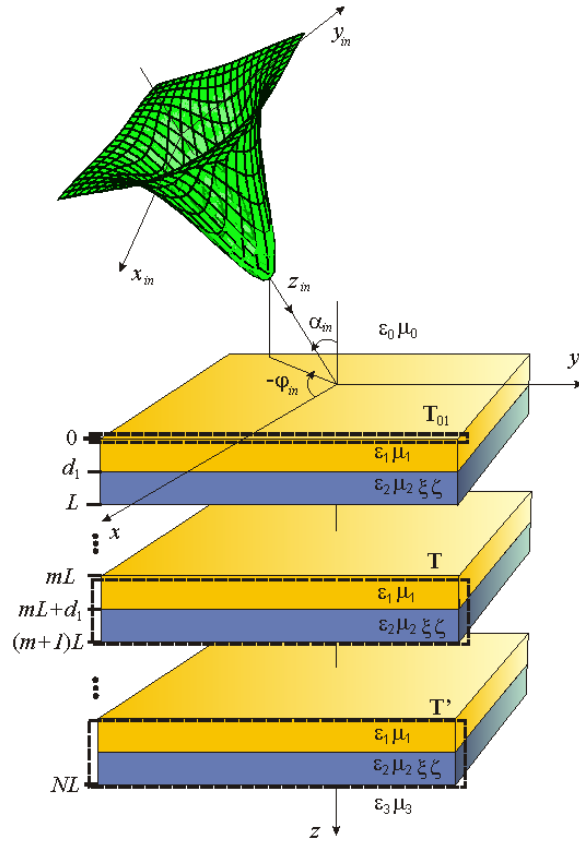


Figure 1. The periodical sequence of bi-isotropic and material layers.

In the equation (1) the vectors are introduced

$$\mathbf{e}_{in} = \mathbf{P}V_p - \mathbf{b}_{in} \times \mathbf{P}V_s, \quad \mathbf{h}_{in} = \mathbf{P}V_s + \mathbf{b}_{in} \times \mathbf{P}V_p. \quad (2)$$

Here the vector \mathbf{P} describes the field polarization,

$$\mathbf{P} = \mathbf{z}_0 \times \mathbf{n}, \quad (3)$$

and in the structure coordinates x, y, z , the vector \mathbf{n} is characterized via the components $(\cos \theta_{in} \cos \varphi_{in}, \cos \theta_{in} \sin \varphi_{in}, 0)$, $\theta_{in} = 90^\circ - \alpha_{in}$, \mathbf{z}_0 is the basis vector of z -axis, and the vector \mathbf{b}_{in} describes the direction of the incident wave beam propagation

$$\mathbf{b}_{in} = \left(\cos \theta_{in} \cos \varphi_{in}, \cos \theta_{in} \sin \varphi_{in}, -\sqrt{\varepsilon_0 \mu_0 - \cos^2 \theta_{in}} \right),$$

$U(\boldsymbol{\kappa}_{in})$ is the spectral density of the beam in the plane $z_{in} = 0$, $\gamma_{in} = \sqrt{k_0^2 - \boldsymbol{\kappa}_{in} \cdot \boldsymbol{\kappa}_{in}}$, $0 < \arg(\sqrt{k_0^2 - \boldsymbol{\kappa}_{in} \cdot \boldsymbol{\kappa}_{in}}) < \pi$ and $\mathbf{a}_{in} = (a_1, a_2)$.

The transformation from the coordinate system x, y, z to x_{in}, y_{in}, z_{in} can be realized via three possibilities: rotating on the angle φ_{in} around the z -axis; rotating on the angle α_{in} around the x -axis; shifting the point of origin to point (a_1, a_2, a_3) . The transition matrix for the first and the second transformations is written in standard view:

$$\begin{bmatrix} x_{in}^0 \\ y_{in}^0 \\ z_{in}^0 \end{bmatrix} = \begin{bmatrix} \cos \varphi_{in} & \sin \varphi_{in} & 0 \\ -\cos \alpha_{in} \sin \varphi_{in} & \cos \alpha_{in} \cos \varphi_{in} & \sin \alpha_{in} \\ \sin \alpha_{in} \sin \varphi_{in} & -\sin \alpha_{in} \cos \varphi_{in} & \cos \alpha_{in} \end{bmatrix} \cdot \begin{bmatrix} x_0 \\ y_0 \\ z_0 \end{bmatrix}. \quad (4)$$

From relations (4) it is continued, that the wave vector components in the mentioned coordinate systems are related in the following way:

$$\begin{bmatrix} \kappa_x \\ \kappa_y \\ \gamma \end{bmatrix} = \begin{bmatrix} \cos \varphi_{in} & -\cos \alpha_{in} \sin \varphi_{in} & \sin \alpha_{in} \sin \varphi_{in} \\ \sin \varphi_{in} & \cos \alpha_{in} \cos \varphi_{in} & -\sin \alpha_{in} \cos \varphi_{in} \\ 0 & \sin \alpha_{in} & \cos \alpha_{in} \end{bmatrix} \cdot \begin{bmatrix} \kappa_{xin} \\ \kappa_{yin} \\ \gamma_{in} \end{bmatrix} \quad (5)$$

or,

$$\begin{bmatrix} \kappa_x \\ \kappa_y \\ \gamma \end{bmatrix} = \begin{bmatrix} \cos \varphi_{in} & -\sin \theta_{in} \sin \varphi_{in} & \cos \theta_{in} \sin \varphi_{in} \\ \sin \varphi_{in} & \sin \theta_{in} \cos \varphi_{in} & -\cos \theta_{in} \cos \varphi_{in} \\ 0 & \cos \theta_{in} & \sin \theta_{in} \end{bmatrix} \cdot \begin{bmatrix} \kappa_{xin} \\ \kappa_{yin} \\ \gamma_{in} \end{bmatrix}, \quad (6)$$

where $\gamma = \sqrt{k_0^2 - \boldsymbol{\kappa} \cdot \boldsymbol{\kappa}}$, $0 < \arg(\sqrt{k_0^2 - \boldsymbol{\kappa} \cdot \boldsymbol{\kappa}}) < \pi$. Taking into account (4) and (5) for the reflected field we have

$$\begin{aligned} \mathbf{E}_{ref} &= \mathbf{U}_{ref}^{ee} + \mathbf{U}_{ref}^{he} \\ &= \mathbf{P}V_e \iint_{-\infty}^{\infty} U(\boldsymbol{\kappa}_{in}) R^{ee}(\boldsymbol{\kappa}) \exp(i\boldsymbol{\kappa} \cdot \mathbf{r} - i\gamma z) d\boldsymbol{\kappa}_{in} \\ &\quad - \mathbf{b}_{ref} \times \mathbf{P}V_h \iint_{-\infty}^{\infty} U(\boldsymbol{\kappa}_{in}) R^{he}(\boldsymbol{\kappa}) \exp(i\boldsymbol{\kappa} \cdot \mathbf{r} - i\gamma z) d\boldsymbol{\kappa}_{in}, \\ \mathbf{H}_{ref} &= \mathbf{U}_{ref}^{hh} + \mathbf{U}_{ref}^{eh} \\ &= \mathbf{P}V_h \iint_{-\infty}^{\infty} U(\boldsymbol{\kappa}_{in}) R^{hh}(\boldsymbol{\kappa}) \exp(i\boldsymbol{\kappa} \cdot \mathbf{r} - i\gamma z) d\boldsymbol{\kappa}_{in} \\ &\quad + \mathbf{b}_{ref} \times \mathbf{P}V_e \iint_{-\infty}^{\infty} U(\boldsymbol{\kappa}_{in}) R^{eh}(\boldsymbol{\kappa}) \exp(i\boldsymbol{\kappa} \cdot \mathbf{r} - i\gamma z) d\boldsymbol{\kappa}_{in}, \end{aligned} \quad (7)$$

and for the transmitted field

$$\begin{aligned}
\mathbf{E}_{tr} &= \mathbf{U}_{tr}^{ee} + \mathbf{U}_{tr}^{he} \\
&= \mathbf{P}V_e \iint_{-\infty}^{\infty} U(\boldsymbol{\kappa}_{in}) \tau^{ee}(\boldsymbol{\kappa}) \exp(i\boldsymbol{\kappa} \cdot \mathbf{r} + i\gamma(z - NL)) d\boldsymbol{\kappa}_{in} \\
&\quad - \mathbf{b}_{tr} \times \mathbf{P}V_h \iint_{-\infty}^{\infty} U(\boldsymbol{\kappa}_{in}) \tau^{he}(\boldsymbol{\kappa}) \exp(i\boldsymbol{\kappa} \cdot \mathbf{r} + i\gamma(z - NL)) d\boldsymbol{\kappa}_{in}, \\
\mathbf{H}_{tr} &= \mathbf{U}_{tr}^{hh} + \mathbf{U}_{tr}^{eh} \\
&= \mathbf{P}V_h \iint_{-\infty}^{\infty} U(\boldsymbol{\kappa}_{in}) \tau^{hh}(\boldsymbol{\kappa}) \exp(i\boldsymbol{\kappa} \cdot \mathbf{r} + i\gamma(z - NL)) d\boldsymbol{\kappa}_{in} \\
&\quad + \mathbf{b}_{ref} \times \mathbf{P}V_e \iint_{-\infty}^{\infty} U(\boldsymbol{\kappa}_{in}) \tau^{eh}(\boldsymbol{\kappa}) \exp(i\boldsymbol{\kappa} \cdot \mathbf{r} + i\gamma(z - NL)) d\boldsymbol{\kappa}_{in},
\end{aligned} \tag{8}$$

In (7) and (8) the reflection $R^{ss'}$ and transmission $\tau^{ss'}$ complex coefficients ($s, s' = e, h$) of the partial plane electromagnetic waves from the structure were introduced. They depend from the frequency of the incident field, angles $(\alpha_{in}, \varphi_{in})$ and the other electromagnetic and geometrical parameters of the structure. The coefficients with coincident indexes (ss) describe the transformation of the incident wave of the perpendicular ($s = e$) or the parallel ($s = h$) polarization into the co-polar wave, and the coefficients with indexes (ss') describe the transformation into the cross-polar wave. The left index corresponds to the incident wave and the right index — to the reflected or transmitted wave. The scattering coefficients $R^{ss'}$ and $\tau^{ss'}$ are determined through the solution of the plane monochromatic wave diffraction problem on the structure under study.

3. TRANSFER MATRIX OF PERIOD. SCATTERING COEFFICIENTS OF PLANE MONOCHROMATIC WAVES

According to the phenomenological description [26, 27], the spatial dispersion effects of the first order are defined via the constitutive equations where the electric and the magnetic inductions are related with the electromagnetic field intensity via the permittivity, permeability and magnetoelectric interaction parameters (the gyration parameters in terms of crystalloptics)

$$\mathbf{D} = \varepsilon_2 \mathbf{E} + \xi \mathbf{H}, \quad \mathbf{B} = \mu_2 \mathbf{H} + \zeta \mathbf{E}, \tag{9}$$

where $\xi = \chi + i\rho$, $\zeta = \chi - i\rho$, χ is a parameter of the nonreciprocity degree of the medium, ρ is the chiral parameter. In a particular case of $\rho \neq 0$, $\chi = 0$ the medium is chiral and reciprocal (the Pasteur

medium), when $\rho = 0$, $\chi \neq 0$ is the nonchiral, nonreciprocal medium (the Tellegen medium).

In the homogeneous along the x -direction bi-isotropic layers, the electromagnetic field is governed by the coupled differential equations

$$\begin{aligned}\Delta_{\perp} E_x + k_0^2 (n_2^2 + \zeta^2) E_x - 2ik_0^2 \rho \mu_2 H_x &= 0, \\ \Delta_{\perp} H_x + k_0^2 (n_2^2 + \xi^2) H_x + 2ik_0^2 \rho \varepsilon_2 E_x &= 0,\end{aligned}\quad (10)$$

where $n_2 = \sqrt{\varepsilon_2 \mu_2}$ is the medium refractive index, and $\Delta_{\perp} = \partial^2 / \partial y^2 + \partial^2 / \partial z^2$.

The waves of the perpendicular ($\mathbf{E}^e \parallel \mathbf{x}_0$) and parallel ($\mathbf{H}^h \parallel \mathbf{x}_0$) linear polarizations can be presented as the superposition of the waves of the right (\mathbf{Q}_s^+) and left (\mathbf{Q}_s^-) circular polarizations [26]:

$$\begin{aligned}E_x^e &= Q_e^+ + Q_e^-, & H_x^e &= -i \left(\frac{1}{\eta_2^+} Q_e^+ - \frac{1}{\eta_2^-} Q_e^- \right), \\ E_x^h &= i (\eta_2^+ Q_h^+ - \eta_2^- Q_h^-), & H_x^h &= Q_h^+ + Q_h^-, \end{aligned}\quad (11)$$

where $\eta_2^{\pm} = \sqrt{\mu_2^{\pm} / \varepsilon_2^{\pm}}$ is the wave impedances of a bi-isotropic medium, $\varepsilon_2^{\pm} = \varepsilon_2 \mp i\xi\eta_2^{-1} \exp(\mp iv)$, $\mu_2^{\pm} = \mu_2 \pm i\zeta\eta_2 \exp(\pm iv)$, $\sin v = (\xi + \zeta) / 2n_2$, $\eta_2 = \sqrt{\mu_2 / \varepsilon_2}$. Such substitution transforms (10) to two independent Helmholtz equations:

$$\Delta_{\perp} Q_s^+ + (\gamma^+)^2 Q_s^+ = 0, \quad \Delta_{\perp} Q_s^- + (\gamma^-)^2 Q_s^- = 0. \quad (12)$$

Here $s = e, h$; $\gamma^{\pm} = k_0 \sqrt{\varepsilon_2^{\pm} \mu_2^{\pm}} = k_0 n_2^{\pm}$ is the propagation constants of the right- (γ^+) (RCP) and left- (γ^-) (LCP) circularly polarized plane wave in the unbounded bi-isotropic medium. Their general solutions for the RCP and LCP waves in a bounded bi-isotropic layer can be written as

$$\begin{aligned}Q_e^{\pm} &= \frac{1}{2\sqrt{Y_2^{e\pm}}} \left\{ A^{e\pm} \exp \left[i \left(\gamma_y^{\pm} y + \gamma_z^{\pm} z \right) \right] + B^{e\pm} \exp \left[i \left(\gamma_y^{\pm} y + \gamma_z^{\pm} z \right) \right] \right\}, \\ Q_h^{\pm} &= \frac{\sqrt{Y_2^{h\pm}}}{2} \left\{ A^{h\pm} \exp \left[i \left(\gamma_y^{\pm} y + \gamma_z^{\pm} z \right) \right] + B^{h\pm} \exp \left[i \left(\gamma_y^{\pm} y - \gamma_z^{\pm} z \right) \right] \right\},\end{aligned}\quad (13)$$

where $A^{s\pm}, B^{s\pm}$ are the wave amplitudes, $Y_2^{e\pm} = \cos \alpha_2^{\pm} / \eta_2^{\pm}$, $Y_2^{h\pm} = (\eta_2^{\pm} \cos \alpha_2^{\pm})^{-1}$ are the wave admittances, $\gamma_y^{\pm} = \gamma^{\pm} \sin \alpha_2^{\pm}$, $\gamma_z^{\pm} = \gamma^{\pm} \cos \alpha_2^{\pm}$, $\sin \alpha_2^{\pm} = \sin \alpha_0 n_0 / n_2^{\pm}$, α_0 are the incidence angle of the partial plane wave on the $z = 0$ structure boundary, α_2^{\pm} are the

refraction angles in the bi-isotropic medium. The substitution (13) to (11) gives the field components of the E - and H -polarizations.

Due to the scattering of the given polarization plane electromagnetic wave (s) by the bi-isotropic layers, the cross-polar components (s') appear in the secondary field. Denote their amplitudes as $A^{s'}$ and $B^{s'}$ for the transmitted and reflected waves, respectively. The field components in the m -th period are shown in the Appendix A.

The structure under study can be considered as a consecutive connection of the eight-poles which are equivalent to the illuminated boundary (\mathbf{T}_{01}), repeated heterogeneity ($\mathbf{T} = \mathbf{T}_1\mathbf{T}_2$) and the last element which is loaded on the waveguide channel having the admittance Y_3^s (\mathbf{T}') (Fig. 1). The equations coupling the field amplitudes at the structure input ($A_0^s, B_0^s, B_0^{s'}$) and output ($A_{N+1}^s, A_{N+1}^{s'}$) for the incident fields of E -type ($A_0^h = 0$) and H -type ($A_0^e = 0$) are obtained as:

$$\begin{pmatrix} A_0^s \\ B_0^s \\ 0 \\ B_0^{s'} \end{pmatrix} = \mathbf{T}_{01}\mathbf{T}^{N-1}\mathbf{T}' \begin{pmatrix} A_{N+1}^s \\ 0 \\ A_{N+1}^{s'} \\ 0 \end{pmatrix}, \quad \begin{pmatrix} A_m^s \\ B_m^s \\ A_m^{s'} \\ B_m^{s'} \end{pmatrix} = \mathbf{T}_1 \begin{pmatrix} A_m^+ \\ B_m^+ \\ A_m^- \\ B_m^- \end{pmatrix},$$

$$\begin{pmatrix} A_{m+1}^+ \\ B_{m+1}^+ \\ A_{m+1}^- \\ B_{m+1}^- \end{pmatrix} = \mathbf{T}_2 \begin{pmatrix} A_{m+1}^s \\ B_{m+1}^s \\ A_{m+1}^{s'} \\ B_{m+1}^{s'} \end{pmatrix}, \quad \begin{pmatrix} A_m^s \\ B_m^s \\ A_m^{s'} \\ B_m^{s'} \end{pmatrix} = \mathbf{T}_1\mathbf{T}_2 \begin{pmatrix} A_{m+1}^s \\ B_{m+1}^s \\ A_{m+1}^{s'} \\ B_{m+1}^{s'} \end{pmatrix}, \quad (14)$$

In [25] it has been shown that $\mathbf{T}_{01}\mathbf{T}^{N-1}\mathbf{T}' = \mathbf{T}_{01}\mathbf{T}^N\mathbf{T}_{13}$, and in the block representation (2×2) the transfer matrices are

$$\mathbf{T}_{pv} = \begin{pmatrix} (\mathbf{T}_{pv}^s) & 0 \\ 0 & (\mathbf{T}_{pv}^{s'}) \end{pmatrix}, \quad \mathbf{T}_1 = \begin{pmatrix} (\mathbf{T}_{1+}^{ss}) & (\mathbf{T}_{1-}^{ss}) \\ (\mathbf{T}_{1+}^{ss'}) & (\mathbf{T}_{1-}^{ss'}) \end{pmatrix}, \quad \mathbf{T}_2 = \begin{pmatrix} (\mathbf{T}_{2+}^{ss}) & (\mathbf{T}_{2+}^{ss'}) \\ (\mathbf{T}_{2-}^{ss}) & (\mathbf{T}_{2-}^{ss'}) \end{pmatrix} \quad (15)$$

where \mathbf{T}_{pv} corresponds to the matrices \mathbf{T}_{01} and \mathbf{T}_{13} . The blocks of the quasi-diagonal matrices are

$$\mathbf{T}_{pv}^s = \frac{1}{2\sqrt{Y_p^s Y_v^s}} \begin{pmatrix} Y_p^s + Y_v^s & \pm(Y_p^s - Y_v^s) \\ \pm(Y_p^s - Y_v^s) & Y_p^s + Y_v^s \end{pmatrix},$$

where the upper sign relates to $s = h$, and the lower sign relates to $s = e$ in terms of the wave types.

The elements of the transfer matrices \mathbf{T}_1 and \mathbf{T}_2 are determined from solving the boundary-value problem and are shown in the Appendix B.

The reflection, transmission and transformation coefficients of the plane monochromatic wave of the reflected ($z \leq 0$) and transmitted ($z \geq NL$) fields are determined by the expressions $R^{ss} = B_0^s/A_0^s$, $\tau^{ss} = A_{N+1}^s/A_0^s$, $R^{ss'} = B_0^{s'}/A_0^s$ and $\tau^{ss'} = A_{N+1}^{s'}/A_0^s$.

The parametrical (including angular) dependences of the scattering coefficients of plane monochromatic waves from the structure with a large number of elements have interleaved areas with the high (the quasi-stop bands) and low (the quasi-pass bands) average level of the reflection (Fig. 2). The interference of the reflected wave from outside boundaries of layers gives $N - 1$ small-scale oscillations in the quasi-pass bands. The maximum of the reflection coefficient magnitude for the cross-polar wave corresponds to the minimum of the reflection coefficient magnitude for the co-polar wave. When the structure is backed by a metal ground plane (the reflecting regime) (Fig. 2(a)), the high- Q resonances of the reflection coefficient magnitude in the quasi-stop bands appear. In the presence of chirality ($\rho \neq 0$) and the dissipation losses ($\text{Im}(\varepsilon_2, \varepsilon_1) \neq 0$), the magnitude of the small-scale oscillations of the reflection coefficient decreases, and the full-resonant transparency vanishes. More detailed analysis of the scattered fields of the partial plane wave on the chiral and material layer sequence is given in [28].

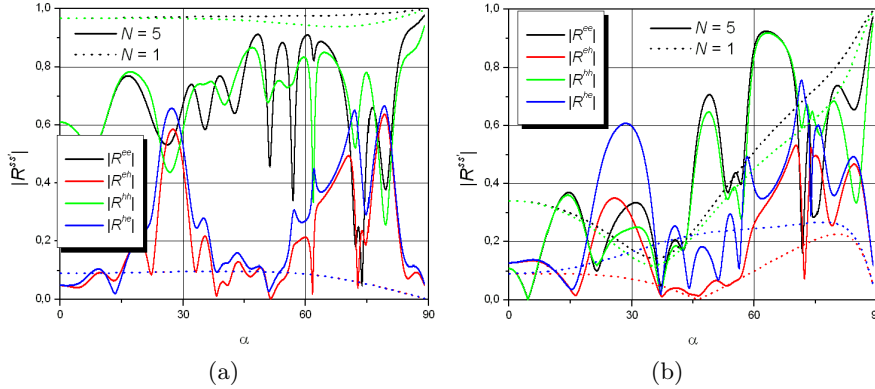


Figure 2. The angular dependences of the reflection coefficient magnitude of the partial plane wave for the sequence of $N = 5$ bi-isotropic and material layers in reflecting (a) and passing (b) regimes: $\varepsilon_0 = \varepsilon_1 = \mu_j = 1$, $j = 0 \div 3$, $k_0L = 10$, $d_1/L = d_2/L = 0.5$, $\rho = \chi = 0.2$; (a) $\varepsilon_2 = 4 + 0.02i$, $\varepsilon_3 \rightarrow \infty$; (b) $\varepsilon_2 = 4$, $\varepsilon_3 = 1$.

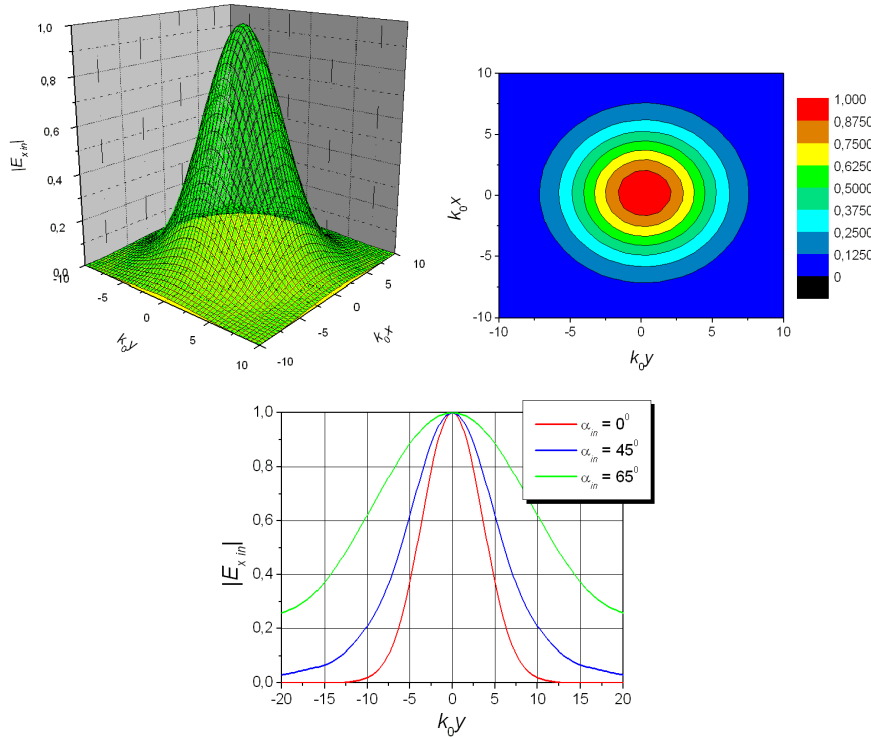


Figure 3. The distribution of the absolute value of the incident beam field in the $z = 0$ plane: $k_0w_x = k_0w_y = 10$, $\varphi_{in} = 0^\circ$.

4. ANALYSIS OF GAUSSIAN BEAM SCATTERING

Let's consider the scattering of a Gaussian beam with the spectral density $U(\boldsymbol{\kappa}_{in})$ that assigns due to law

$$U(\boldsymbol{\kappa}_{in}) = \exp\left(-(\boldsymbol{w} \cdot \boldsymbol{\kappa}_{in})^2/16\right) H_n\left(k_{xin}w_x/\sqrt{2}\right) H_m\left(k_{yin}w_y/\sqrt{2}\right) \quad (16)$$

where $\boldsymbol{w} = (w_x, w_y)$, w_x and w_y are beam widths along x_{in} and y_{in} axis, respectively, $H_n(\cdot)$ is the Hermit polynomial of n -th order. Restrict oneself to case of the zeroth-order ($n = m = 0$) beam (Fig. 3).

Some effects, like the beam form distortion, ellipticity change, beam splitting, lateral shift were discovered in the scattered beam (Figs. 4–6). Those effects are connected to the angular dependence of the phase and magnitude of the co-polar $|R^{ss}|$ and the cross-polar $|R^{ss'}$ component of the partial plane wave reflection coefficients (Fig. 2).

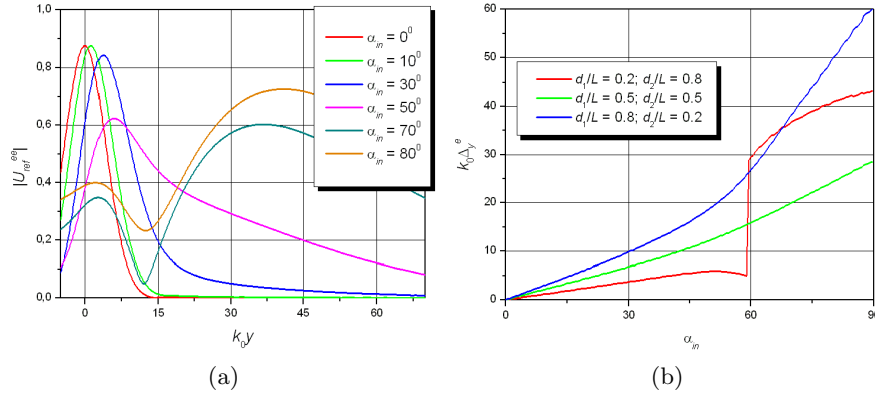
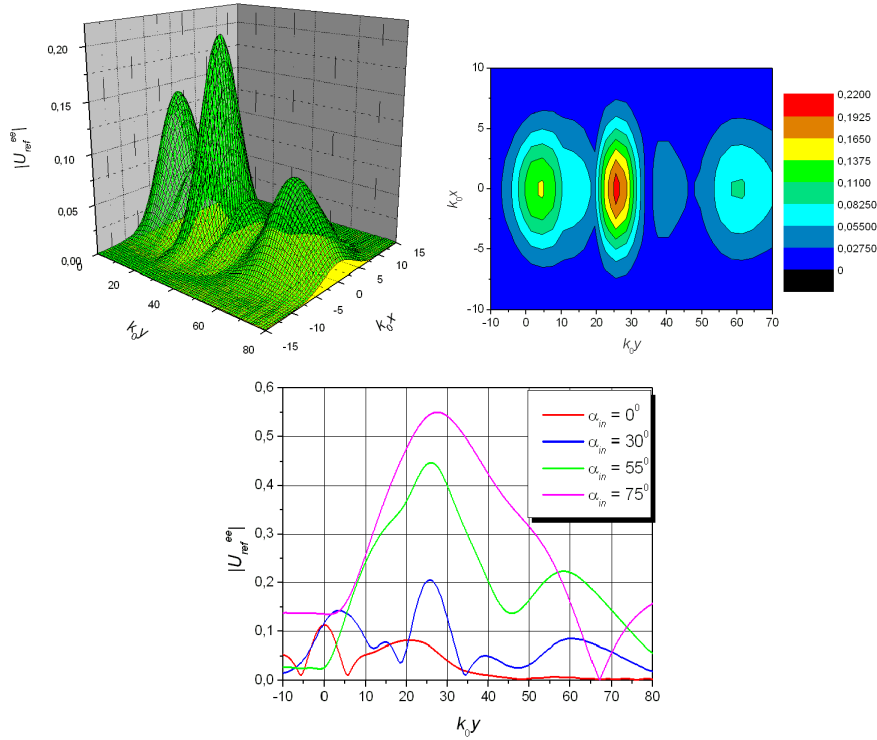
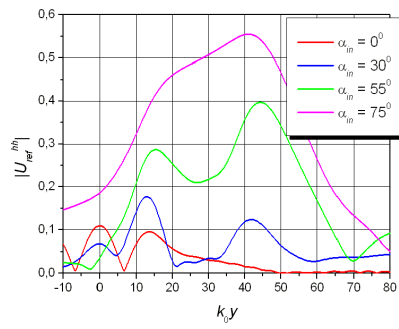
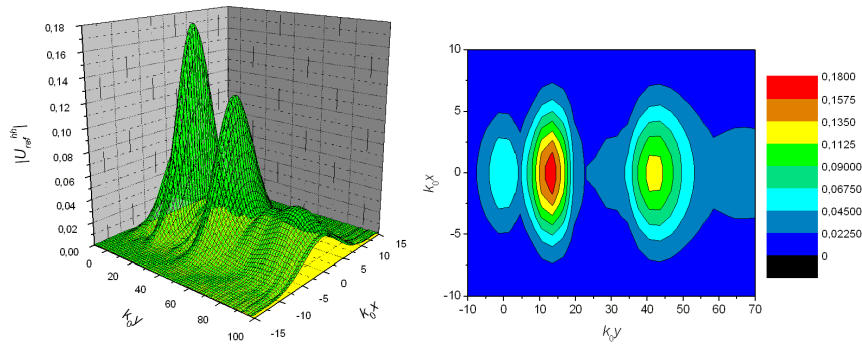
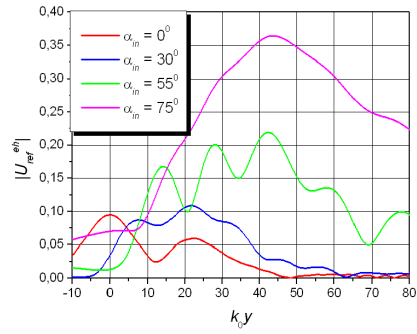
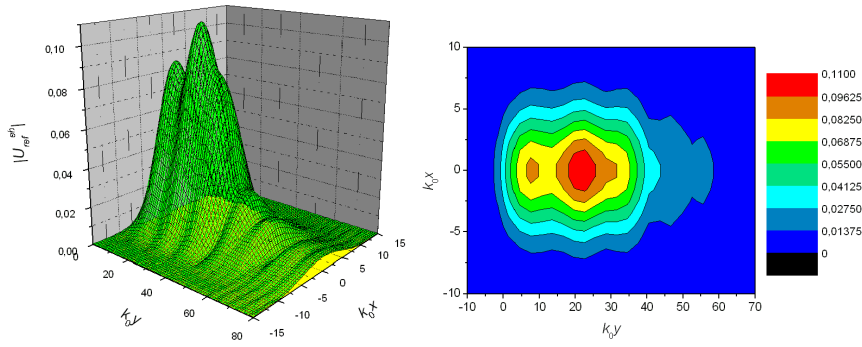


Figure 4. The distribution of the absolute value of the field (a) and the lateral shift value of its maximum (b) of the reflected wave beam in the $z = 0$ plane for the structure that includes single isotropic and single bi-isotropic layers ($N = 1$): $\varepsilon_0 = \varepsilon_1 = \mu_j = 1$, $j = 0 \div 3$, $\varepsilon_2 = 4 + 0.02i$, $\varepsilon_3 \rightarrow \infty$, $k_0L = k_0w = k_0b = 10$, $\rho = \chi = 0.2$, $\varphi_{in} = 0^\circ$; (a) $d_1/L = 0.2$, $d_2/L = 0.8$.





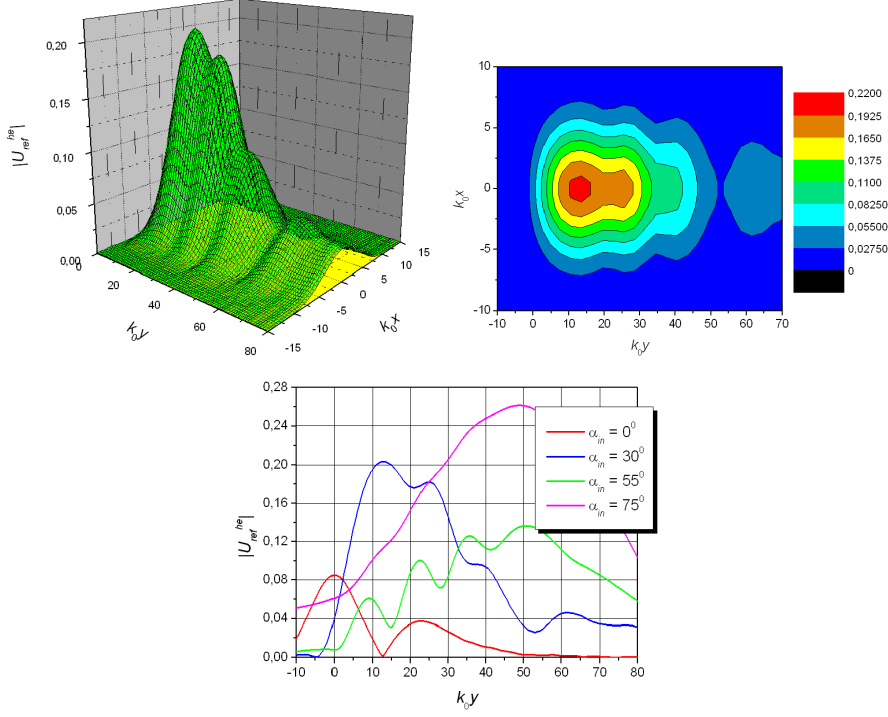
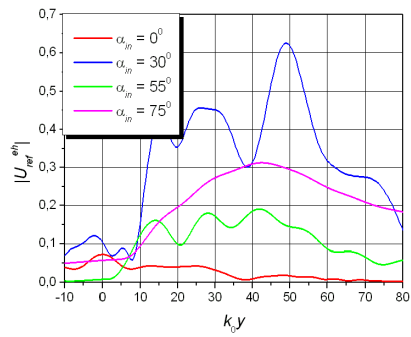
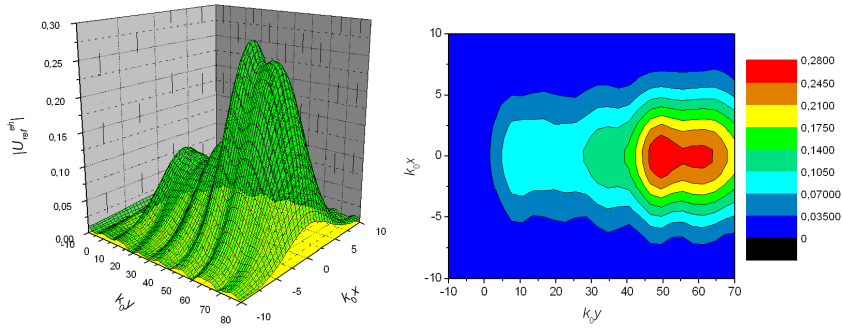
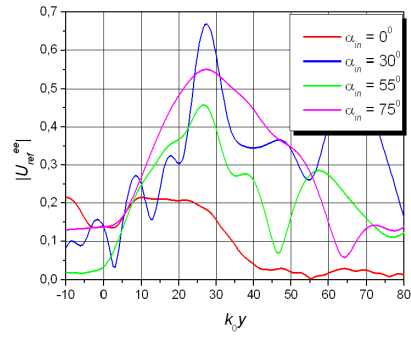
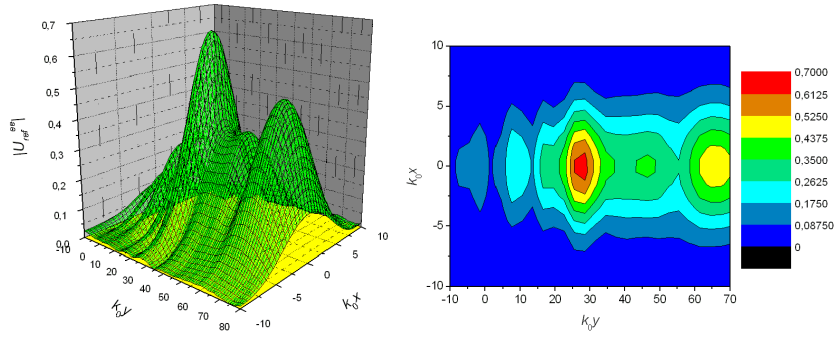


Figure 5. The distribution of the absolute value of the field $|U_{ref}|$ of the reflected wave beam in the $z = 0$ plane for the sequence of $N = 5$ isotropic and bi-isotropic layers (the passing regime): $\varepsilon_0 = \varepsilon_1 = \mu_j = 1$, $j = 0 \div 3$, $\varepsilon_2 = 4$, $k_0L = k_0w = k_0b = 10$, $d_1/L = d_2/L = 0.5$, $\rho = \chi = 0.2$.

If the structure includes the single basic element ($N = 1$) and is backed by a metal ground plane, the reflection coefficient magnitude of the co-polar wave $|R^{ss}|$ is weakly depend from the falling angle and is nearly per unit (Fig. 2a). When $\varphi_{in} = 0$, for the two-dimensional beam, during [1], the field components U_{ref}^{ee} and U_{ref}^{hh} of the reflected beam have the next view

$$\begin{aligned}
 U_{ref}^{ss}(y, z) = & \exp\{i\Phi^{ss}(\kappa_0)\} R^{ss}(\kappa_0) V_s \\
 & \times \int_{-\infty}^{\infty} U(\kappa_{in}) \exp\left\{i\left[(\kappa_{in} - \kappa_0)(y + \Delta_y^s) - i\gamma z\right]\right\} d\kappa_{in},
 \end{aligned} \tag{17}$$

where $\kappa_0 = k \sin \alpha_{in}$ and $\Phi^{ss}(\kappa_0)$ is the phase of the reflection



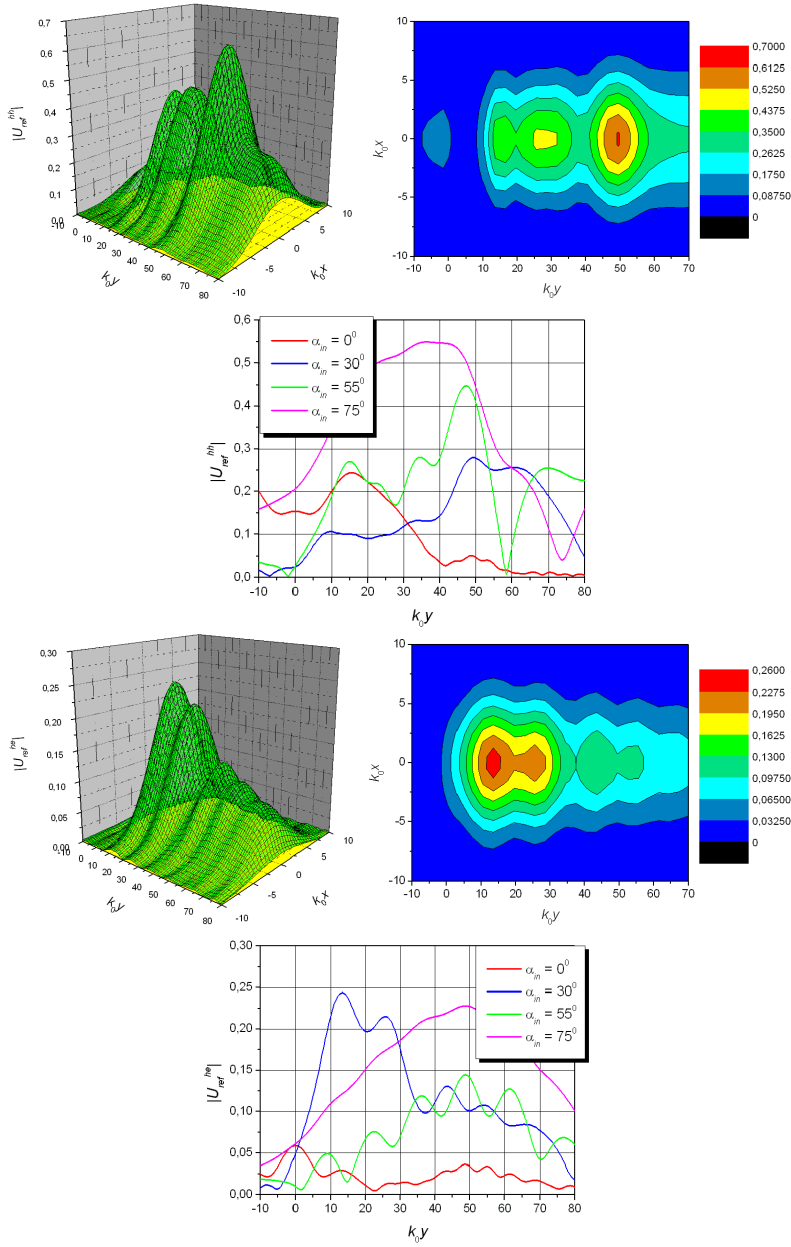


Figure 6. The distribution of the absolute value of the field $|U_{ref}|$ of the reflected wave beam in the $z = 0$ plane for the sequence of $N = 5$ isotropic and bi-isotropic layers (the reflecting regime): $\varepsilon_0 = \varepsilon_1 = \mu_j = 1$, $j = 0 \div 3$, $\varepsilon_2 = 4 + 0.02j$, $\varepsilon_3 \rightarrow \infty$, $k_0L = k_0w = k_0b = 10$, $d_1/L = d_2/L = 0.5$, $\rho = \chi = 0.2$, $\alpha_{in} = 30^\circ$.

coefficient of the partial wave which falls under an angle α_{in} . The scattered beam shift along the illuminated boundary of the structure is defined from the condition $\Delta_y^s = -(\partial\Phi^{ss}/\partial\kappa)_{\kappa=\kappa_0}$. It is sizeable when the phase of the partial plane wave scattering coefficient rapidly changes with the angle. When the angle of the falling beam is nearly to the quasi-Brewster angle or greater then it, the splitting of the reflected beam into two beams with different intensity value appears (Fig. 4).

When $N > 1$, the shift of the reflected beam along the illuminated boundary of the structure increases due to multiple reflections of waves from the boundaries of the layers (Figs. 5, 6). The beam splitting is observed on the angles that lie nearly of the totally transmission angles of the partial plane wave.

Increasing the chiral parameter ρ raises the structure reflection, changes the ellipticity and slightly raises the lateral shift of the reflected beam. The maximum of the intensity for the cross-polar wave corresponds to the minimum of the intensity for the co-polar wave. There are the areas of the practically totally transformation of the co-polar wave into the cross-polar wave. To the presence of the media nonreciprocity ($\chi \neq 0$) is $|U^{eh}| \neq |U^{he}|$ and the sizeable cross-polar component in the scattered field appears even for case of the straight incident wave beam ($\alpha_{in} = 0^\circ$).

We would like to emphasize an important peculiarity of the system under study regarding its application in the design of high-precision matched loads and layered absorbing coatings (Fig. 6) [24, 25, 29]. This peculiarity consists in reducing the co-polar reflection due to wave transformation into the cross-polar reflection.

5. CONCLUSION

In this paper, we have investigated the tree-dimensional Gaussian beam scattering for the DBR-like bounded periodic sequence of pairs of bi-isotropic and magnetodielectric layers. The lateral shift, ellipticity change, beam splitting is studied. The revealed effects allows us to recommend the application of the studied structure in the design of cascaded high- Q and stop-band frequency filters, wave transformers, angular discriminators, absorbers, etc.

APPENDIX A.

With $z_m = mL$, $z_{m1} = mL + d_1$, notations, the field components in the m -th period of the structure $z_m \leq z \leq z_{m1}$ and $z_{m1} \leq z \leq (m + 1)L$

are written as follows (the factor $\exp[-i(\omega t - k_y y)]$ is omitted):

$$\begin{aligned} \begin{Bmatrix} E_{x1}^e \\ E_{y1}^h \end{Bmatrix} &= \pm \begin{Bmatrix} 1/\sqrt{Y_1^e} \\ i/\sqrt{Y_1^h} \end{Bmatrix} \\ &\times \left(\begin{Bmatrix} A_m^e \\ A_m^h \end{Bmatrix} \exp[ik_{z1}(z - z_m)] \pm \begin{Bmatrix} B_m^e \\ B_m^h \end{Bmatrix} \exp[-ik_{z1}(z - z_m)] \right), \\ \begin{Bmatrix} H_{y1}^e \\ H_{x1}^h \end{Bmatrix} &= \begin{Bmatrix} \sqrt{Y_1^e} \\ i\sqrt{Y_1^h} \end{Bmatrix} \\ &\times \left(\begin{Bmatrix} A_m^e \\ A_m^h \end{Bmatrix} \exp[ik_{z1}(z - z_m)] \mp \begin{Bmatrix} B_m^e \\ B_m^h \end{Bmatrix} \exp[-ik_{z1}(z - z_m)] \right), \\ \begin{Bmatrix} E_{x2} \\ E_{y2} \end{Bmatrix} &= \pm \begin{Bmatrix} 1/2\sqrt{Y_2^{e+}} \\ i/2\sqrt{Y_2^{h+}} \end{Bmatrix} (A_m^+ \exp[i\gamma_z^+(z - z_{m1})] \pm B_m^+ \exp[-i\gamma_z^+(z - z_{m1})]) \\ &+ \begin{Bmatrix} 1/2\sqrt{Y_1^{e-}} \\ i/2\sqrt{Y_1^{h-}} \end{Bmatrix} (A_m^- \exp[i\gamma_z^-(z - z_{m1})] \pm B_m^- \exp[-i\gamma_z^-(z - z_{m1})]), \\ \begin{Bmatrix} H_{y2} \\ H_{x2} \end{Bmatrix} &= \begin{Bmatrix} \sqrt{Y_2^{e+}}/2 \\ i\sqrt{Y_2^{h+}}/2 \end{Bmatrix} (A_m^+ \exp[i\gamma_z^+(z - z_{m1})] \mp B_m^+ \exp[-i\gamma_z^+(z - z_{m1})]) \\ &\pm \begin{Bmatrix} \sqrt{Y_2^{e-}}/2 \\ i\sqrt{Y_2^{h-}}/2 \end{Bmatrix} (A_m^- \exp[i\gamma_z^-(z - z_{m1})] \mp B_m^- \exp[-i\gamma_z^-(z - z_{m1})]), \end{aligned}$$

The field components at the structure output are

$$\begin{aligned} \begin{Bmatrix} E_{x3}^e \\ E_{y3}^h \end{Bmatrix} &= \pm \begin{Bmatrix} (1/\sqrt{Y_3^e}) A_{N+1}^e \\ (i/\sqrt{Y_3^h}) A_{N+1}^h \end{Bmatrix} \exp[ik_{z3}(z - NL)], \\ \begin{Bmatrix} H_{y3}^e \\ H_{x3}^h \end{Bmatrix} &= \pm \begin{Bmatrix} \sqrt{Y_3^e} A_{N+1}^e \\ i\sqrt{Y_3^h} A_{N+1}^h \end{Bmatrix} \exp[ik_{z3}(z - NL)]. \end{aligned}$$

Here $k_{zj} = k_j \cos \alpha_j$, $k_{yj} = k_j \sin \alpha_j$, $k_j = k_0 n_j$, $n_j = \sqrt{\varepsilon_j \mu_j}$, $Y_j^e = \eta_j^{-1} \cos \alpha_j$, $Y_j^h = (\eta_j \cos \alpha_j)^{-1}$, $\eta_j = \sqrt{\mu_j / \varepsilon_j}$, $\sin \alpha_j = \sin \alpha_0 n_0 / n_j$ and $j \neq 2$.

APPENDIX B.

The elements of the transfer matrix $\mathbf{T} = \mathbf{T}_1 \mathbf{T}_2$ are:

$$\begin{aligned}
\mathbf{T}_{1\pm}^{ee} &= \frac{1}{2\sqrt{Y_1^e Y_2^{e\pm}}} \begin{pmatrix} Y_1^e + Y_2^{e\pm} & Y_1^e - Y_2^{e\pm} \\ Y_1^e - Y_2^{e\pm} & Y_1^e + Y_2^{e\pm} \end{pmatrix} \mathbf{E}_1, \\
\mathbf{T}_{1\pm}^{eh} &= \pm \frac{1}{2\sqrt{Y_1^h Y_2^{h\pm}}} \begin{pmatrix} Y_2^{h\pm} + Y_1^h & Y_2^{h\pm} - Y_1^h \\ Y_2^{h\pm} - Y_1^h & Y_2^{h\pm} + Y_1^h \end{pmatrix} \mathbf{E}_1, \\
\mathbf{T}_{1\pm}^{hh} &= \frac{1}{2\sqrt{Y_1^h Y_2^{h\pm}}} \begin{pmatrix} Y_2^{h\pm} + Y_1^h & Y_2^{h\pm} - Y_1^h \\ Y_2^{h\pm} - Y_1^h & Y_2^{h\pm} + Y_1^h \end{pmatrix} \mathbf{E}_1, \\
\mathbf{T}_{1\pm}^{he} &= \mp \frac{1}{2\sqrt{Y_1^e Y_2^{e\pm}}} \begin{pmatrix} Y_1^e + Y_2^{e\pm} & Y_1^e - Y_2^{e\pm} \\ Y_1^e - Y_2^{e\pm} & Y_1^e + Y_2^{e\pm} \end{pmatrix} \mathbf{E}_1, \\
\mathbf{T}_{2\pm}^{ee} &= \frac{1}{4Y_2^{e\mp} \sqrt{Y_1^e Y_2^{e\pm}}} \\
&\times \begin{pmatrix} (Y_2^{e\mp} + Y_1^e)(Y_2^{e\mp} + Y_2^{e\pm}) - (Y_2^{e\mp} - Y_1^e)(Y_2^{e\mp} - Y_2^{e\pm}) \\ (Y_2^{e\mp} - Y_1^e)(Y_2^{e\mp} + Y_2^{e\pm}) - (Y_2^{e\mp} + Y_1^e)(Y_2^{e\mp} - Y_2^{e\pm}) \\ (Y_2^{e\mp} - Y_1^e)(Y_2^{e\mp} + Y_2^{e\pm}) - (Y_2^{e\mp} + Y_1^e)(Y_2^{e\mp} - Y_2^{e\pm}) \\ (Y_2^{e\mp} + Y_1^e)(Y_2^{e\mp} + Y_2^{e\pm}) - (Y_2^{e\mp} - Y_1^e)(Y_2^{e\mp} - Y_2^{e\pm}) \end{pmatrix} \mathbf{E}_2^{\pm}, \\
\mathbf{T}_{2\pm}^{eh} &= \mp \frac{1}{4Y_2^{h\mp} \sqrt{Y_1^h Y_2^{h\pm}}} \\
&\times \begin{pmatrix} (Y_2^{h\mp} + Y_1^h)(Y_2^{h\mp} + Y_2^{h\pm}) - (Y_2^{h\mp} - Y_1^h)(Y_2^{h\mp} - Y_2^{h\pm}) \\ (Y_2^{h\mp} + Y_1^h)(Y_2^{h\mp} - Y_2^{h\pm}) - (Y_2^{h\mp} - Y_1^h)(Y_2^{h\mp} + Y_2^{h\pm}) \\ (Y_2^{h\mp} + Y_1^h)(Y_2^{h\mp} - Y_2^{h\pm}) - (Y_2^{h\mp} - Y_1^h)(Y_2^{h\mp} + Y_2^{h\pm}) \\ (Y_2^{h\mp} + Y_1^h)(Y_2^{h\mp} + Y_2^{h\pm}) - (Y_2^{h\mp} - Y_1^h)(Y_2^{h\mp} - Y_2^{h\pm}) \end{pmatrix} \mathbf{E}_2^{\pm}, \\
\mathbf{T}_{2\pm}^{hh} &= \frac{1}{4Y_2^{h\mp} \sqrt{Y_1^h Y_2^{h\pm}}} \\
&\times \begin{pmatrix} (Y_2^{h\mp} + Y_1^h)(Y_2^{h\mp} + Y_2^{h\pm}) - (Y_2^{h\mp} - Y_1^h)(Y_2^{h\mp} - Y_2^{h\pm}) \\ (Y_2^{h\mp} + Y_1^h)(Y_2^{h\mp} - Y_2^{h\pm}) - (Y_2^{h\mp} - Y_1^h)(Y_2^{h\mp} + Y_2^{h\pm}) \\ (Y_2^{h\mp} + Y_1^h)(Y_2^{h\mp} - Y_2^{h\pm}) - (Y_2^{h\mp} - Y_1^h)(Y_2^{h\mp} + Y_2^{h\pm}) \\ (Y_2^{h\mp} + Y_1^h)(Y_2^{h\mp} + Y_2^{h\pm}) - (Y_2^{h\mp} - Y_1^h)(Y_2^{h\mp} - Y_2^{h\pm}) \end{pmatrix}
\end{aligned}$$

$$\begin{aligned}
& \left(\begin{array}{l} (Y_2^{h\mp} + Y_1^h) (Y_2^{h\mp} - Y_2^{h\pm}) - (Y_2^{h\mp} - Y_1^h) (Y_2^{h\mp} + Y_2^{h\pm}) \\ (Y_2^{h\mp} + Y_1^h) (Y_2^{h\mp} + Y_2^{h\pm}) - (Y_2^{h\mp} - Y_1^h) (Y_2^{h\mp} - Y_2^{h\pm}) \end{array} \right) \mathbf{E}_2^\pm, \\
\mathbf{T}_{2\pm}^{he} = & \mp \frac{1}{4Y_2^{e\mp} \sqrt{Y_1^e Y_2^{e\pm}}} \\
& \times \left(\begin{array}{l} (Y_2^{e\mp} + Y_1^e) (Y_2^{e\mp} + Y_2^{e\pm}) - (Y_2^{e\mp} - Y_1^e) (Y_2^{e\mp} - Y_2^{e\pm}) \\ (Y_2^{e\mp} - Y_1^e) (Y_2^{e\mp} + Y_2^{e\pm}) - (Y_2^{e\mp} + Y_1^e) (Y_2^{e\mp} - Y_2^{e\pm}) \\ (Y_2^{e\mp} - Y_1^e) (Y_2^{e\mp} + Y_2^{e\pm}) - (Y_2^{e\mp} + Y_1^e) (Y_2^{e\mp} - Y_2^{e\pm}) \\ (Y_2^{e\mp} + Y_1^e) (Y_2^{e\mp} + Y_2^{e\pm}) - (Y_2^{e\mp} - Y_1^e) (Y_2^{e\mp} - Y_2^{e\pm}) \end{array} \right) \mathbf{E}_2^\pm,
\end{aligned}$$

where

$$\begin{aligned}
\mathbf{E}_1 &= \text{Diag}(\exp(-ik_{z1}d_1) \exp(ik_{z1}d_1)), \\
\mathbf{E}_2^\pm &= \text{Diag}(\exp(-i\gamma_z^\pm d_2) \exp(i\gamma_z^\pm d_2)).
\end{aligned}$$

REFERENCES

1. Brekhovskikh, L. M., *Waves in Layered Media*, Academic Press, New York, 1960.
2. Goncharenko, A. M., *Gaussian Beams of Light*, Minsk, Nauka & Tekhnika, 1977 (in Russian).
3. Horowitz, B. R. and T. Tamir, "Lateral displacement of a light beam at a dielectric interface," *J. Opt. Soc. Am.*, Vol. 61, 584–594, 1971.
4. Tretyakova, S. S., O. A. Tretyakov, V. P. Shestopalov, "Wave beam diffraction on plane periodical structures," *Radiotekhnika & Electronica*, Vol. 17, 1366–1373, July 1972 (in Russian).
5. Shin, S. Y. and L. B. Felsen, "Lateral shift of totally reflected Gaussian beams," *Radio Sci.*, Vol. 12, 551–564, July 1977.
6. Godin, O. A., "Diffraction theory of lateral shift of bounded wave beams during reflection," *Zh. Tekh. Fiz., Part 1*, Vol. 54, 2094–2104, 1984; Part 2, Vol. 55, 17–25, 1985 (in Russian).
7. Riesz, R. P. and R. Simon, "Reflection of Gaussian beam from a dielectric slab," *J. Opt. Soc. Am. A*, Vol. 2, 1809–1817, 1985.
8. Maciel, J. and L. Felsen, "Gaussian beam analysis of propagation from an extended plane aperture distribution through dielectric layers," *IEEE Trans. Antennas Propagat.*, Vol. AP-38, 1607–1624, October 1990.

9. Shulga, S. N., "Two-dimensional wave beam scattering on an anisotropic half-space with anisotropic inclusion," *Optics & Spectroscopy*, Vol. 87, 503–509, March 1999 (in Russian).
10. Tuz, V. R., "Gaussian beam scattering from a bounded periodic sequence of perfectly conducting bars," *Radiotekhnika*, Vol. 135, 62–67, 2003 (in Russian).
11. Bass, F. and L. Resnick, "Wave beam propagation in layered media," *Journal of Electromagnetic Waves and Applications*, Vol. 17, No. 3, 479–480, 2003.
12. Lomakin, V. and E. Michielssen, "Beam transmission through periodic subwavelength hole structures," *IEEE Trans. Antennas Propagat.*, Vol. AP-55, 1564–1581, June 2007.
13. Hoppe, D. J. and Y. Rahmat-Samii, "Gaussian beam reflection at a dielectric-chiral interface," *Journal of Electromagnetic Waves and Applications*, Vol. 6, 603–624, 1992.
14. Maksimenko, S. A., G. Ya. Slepyan, and A. Lakhtakia, "Gaussian pulse propagation in a linear, lossy, chiral medium," *J. Opt. Soc. Am. A*, Vol. 14, 894–900, April 1997.
15. Maksimenko, S. A. and G. Ya. Slepyan, "Pulse propagation in linear and nonlinear chiral media," *Int. Conf. and Workshop on Electromag. Complex Media, BIANISOTROPICS'97*, Glasgow, Scotland, June 5–7, 1997.
16. Mahmoud, S. F. and S. Tariq, "Gaussian beam splitting by a chiral prism," *Journal of Electromagnetic Waves and Applications*, Vol. 2, 73–83, January 1998.
17. Malyuskin, A. V., D. N. Goryushko, S. N. Shulga, A. A. Shmat'ko, "Scattering of a wave beam by inhomogeneous anisotropic chiral layer," *Int. Conf. on Math. Methods in EM Theory (MMET 2002)*, 566–568, Kyiv, Ukraine, September 10–13, 2002.
18. Kopp, V. I., Z.-Q. Zhang, and A. Z. Genack, "Lasing in chiral photonic structures," *Prog. Quantum Electron.*, Vol. 27, 369–416, June 2003.
19. Ghosh, A. and P. Fischer, "Chiral molecules split light: reflection and refraction in a chiral liquid," *Phys. Rev. Lett.*, Vol. 97, 2006.
20. Luk, K. M. and A. L. Cullen, "Three-dimensional Gaussian beam reflection from short-circuited isotropic ferrite slab," *IEEE Trans. Antennas Propagat.*, Vol. 41, 962–966, July 1993.
21. Born, M. and E. Wolf, *Principle of Optics*, Oxford, Pergamon Press, 1968.
22. Zhang, Y. J., A. Bauer, and E. P. Li, "T-Matrix analysis of multiple scattering from parallel semi-circular channels filled with

- ciral media in a conducting plane,” *Progress In Electromagnetics Research*, PIER 53, 299–318, 2005.
23. Kim, G. and E. Garmire, “Comparison between the matrix method and the coupled-wave method in the analysis of Bragg reflector structures,” *J. Opt. Soc. Am. A*, Vol. 9, 132–137, 1992.
 24. Kazanskiy, V. B. and V.V. Podlozny, “Quasiperiodic layered structure with resistive film,” *Electromagnetics*, Vol. 17, 131–145, March–April 1997.
 25. Kazanskiy, V. B., V. R. Tuz, and V. V. Khardikov, “Quasiperiodic metal-dielectric structure as a multifunctional control system,” *Radioelectronics and Communications Systems*, Vol. 45, 38–46, July 2002.
 26. Lindell, I. V., A. H. Sihvola, S. A. Tretyakov, and A. J. Viitanen, *Electromagnetic Waves in Chiral and Bi-Isotropic Media*, Artech House, Boston, London, 1994.
 27. Lakhtakia, A., V. K. Varadan, and V. V. Varadan, *Time-Harmonic Electromagnetic Fields in Chiral Media, Lecture Notes in Physics*, Springer-Verlag, 1989.
 28. Kazanskiy, V. B. and V. R. Tuz, “Scattering fields of Chiral layers periodical sequence,” *Int. Conference on Antenna Theory and Tech.*, 177–180, Sevastopol, Ukraine, September 17–21, 2007.
 29. Norgen, M., “On the possibility of reflectionless coating of a homogeneous bianisotropic layer on a perfect conductor,” *Electromagnetics*, Vol. 17, 295–307, April 1997.
 30. Varadan, V. K., Y. Ma, and V. V. Varadan, “Microwave properties of chiral composites,” *Progress In Electromagnetics Research*, PIER 6, 327–344, 1992.
 31. Mariotte, F., P. Pelet, and N. Engeta, “A review of recent study of guided waves in chiral media,” *Progress In Electromagnetics Research*, PIER 9, 311–350, 1994.
 32. Komar, G. I. and A. Y. Poyedinchuk, “Mode transfigurations in chirowaveguides,” *Journal of Electromagnetic Waves and Applications*, Vol. 17, No. 7, 1043–1044, 2003.
 33. Zheng, L. G. and W. X. Zhang, “Analysis of bi-anisotropic PBG structure using plane wave expansion method,” *Journal of Electromagnetic Waves and Applications*, Vol. 17, No. 10, 1419–1420, 2003.
 34. Hussain, A. and Q. A. Naqvi, “Fractional curl operator in chiral medium and fractional non-symmetric transmission line,” *Progress In Electromagnetics Research*, PIER 59, 199–213, 2006.
 35. Panin, S. B., P. D. Smith, and A. Y. Poyedinchuk, “Elliptical

- to linear polarization transformation by a grating on a chiral medium,” *Journal of Electromagnetic Waves and Applications*, Vol. 21, No. 13, 1885–1899, 2007.
36. Kuzu, L., V. Demir, A. Z. Elsherbeni, and E. Arvas, “Electromagnetic scattering from arbitrarily shaped chiral objects using the finite difference frequency domain method,” *Progress In Electromagnetics Research*, PIER 67, 1–24, 2007.
 37. Hussain, A., M. Faryad, and Q. A. Naqvi, “Fractional curl operator and fractional chiro-waveguide,” *Journal of Electromagnetic Waves and Applications*, Vol. 21, No. 8, 1119–1129, 2007.